

# Charge and Sodium Ordering in $\beta\text{-Na}_{0.33}\text{V}_2\text{O}_3$

P. H. M. van Loosdrecht,<sup>1</sup> C. N. Presura,<sup>1</sup> M. Popinciuc,<sup>1</sup> D. van der Marel,<sup>1</sup> G. Maris,<sup>1</sup>  
T. T. M. Palstra,<sup>1</sup> P. J. M. van Bentum,<sup>2</sup> H. Yamada,<sup>3</sup> T. Yamauchi,<sup>3</sup> and Y. Ueda<sup>3</sup>

---

Polarized Raman and optical spectra for the quasi one-dimensional metallic vanadate  $\beta\text{-Na}_{0.33}\text{V}_2\text{O}_3$  are reported for various temperatures. The spectra are discussed in the light of the sodium and charge ordering transitions occurring in this material, and demonstrate the presence of strong electron-phonon coupling.

---

**KEY WORDS:** charge ordering; metal-insulator transition; vanadates; phase transitions; Raman and optical spectroscopy.

## 1. INTRODUCTION

The recent discovery [1] of a clear metal-insulator transition (MIT) in the vanadium bronze  $\beta\text{-Na}_{0.33}\text{V}_2\text{O}_3$  has sparked a revival of interest in this quasi one-dimensional(1D) metallic system. In addition to the MIT,  $\beta\text{-Na}_{0.33}\text{V}_2\text{O}_3$  undergoes a structural sodium ordering transition at higher temperatures, a magnetic transition at low temperatures, and a transition into a superconducting state under high pressure [2]. Several important aspects of this 1D material have remained unclear, including the nature of the spin and charge excitations, and the relation between the Na ordering and the MIT. This contribution presents a Raman and optical study of  $\beta\text{-Na}_{0.33}\text{V}_2\text{O}_3$  focusing on the various phase transitions and electron-phonon coupling in this compound.

## 2. STRUCTURE AND PHASE TRANSITIONS

At room temperature  $\beta\text{-Na}_{0.33}\text{V}_2\text{O}_3$  has a monoclinic structure (spacegroup  $C_{2h}^2$ ,  $a = 10.08 \text{ \AA}$ ,  $b = 3.61 \text{ \AA}$ ,  $c = 15.44 \text{ \AA}$ ,  $\beta = 109.6^\circ$ ) [3,4]. The structure consists of zigzag double chains of  $\text{VO}_6$  octahedra,

forming sheets by joining corners. These sheets are separated by additional chains of double  $\text{VO}_5$  trigonal bipyramids, giving rise to unidirectional tunnels along **b** (see Fig. 1) in which the Na ions are located. At a sodium stoichiometry of 0.33, there is exactly one sodium atom per primitive cell. The sodium ion can occupy two closely spaced positions, although simultaneous occupation of the two sites is prohibited (the distance between the sites is  $1.95 \text{ \AA}$ ). NMR experiments [5] suggest that, at room temperature, the occupation of these two sites is random, giving rise to a disordered structure. At  $T \simeq 240 \text{ K}$  a second-order phase transition occurs in which the sodium atoms order in a zigzag fashion along the unique axis accompanied by a doubling of the *b*-axis [1]. Two additional transitions occur at lower temperatures. At  $T \simeq 136 \text{ K}$  an MIT has been observed, in which the unit cell undergoes an additional tripling along the *b*-axis [6]. It has been suggested that the charge ordering occurs because of a localization of the charge on chains along the *b*-direction formed by the  $\text{V}_1$  ions. Finally, at  $T \simeq 22 \text{ K}$  there is a transition from the paramagnetic high-temperature state to a canted antiferromagnetic state [7].

## 3. RAMAN SPECTROSCOPY

The samples used in this study have been prepared as described in [1]. Typical sizes are 5–6 mm along the *b*-direction and about 0.3–1 mm in the other two directions. For the Raman experiments, samples

<sup>1</sup>Material Science Center, University of Groningen, Nijenborgh 4, 9747 AG Groningen, The Netherlands.

<sup>2</sup>University of Nijmegen, Toernooiveld, 6525 ED Nijmegen, The Netherlands.

<sup>3</sup>Institute for Solid State Physics, University of Tokyo, Tokyo, Japan.

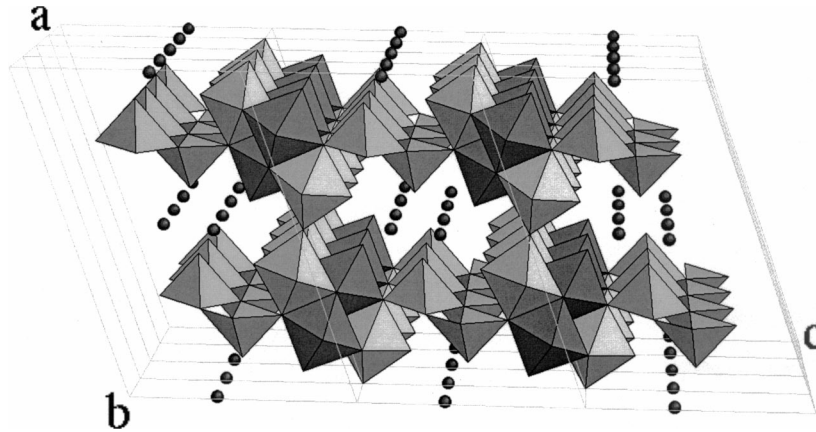


**Fig. 1.** Room temperature structure of  $\beta\text{-Na}_{0.33}\text{V}_2\text{O}_3$  showing chains of  $\text{V}_1$  (dark octahedra),  $\text{V}_2$  (light octahedra), and  $\text{V}_3$  ions (pyramids).

were mounted in a flow cryostat (stabilization better than 1 K). Polarized spectra have been recorded in a back reflection geometry using an  $\text{Ar}^+$  ion laser (514 nm) for excitation (power  $<5$  mW, spot size  $100\ \mu\text{m}$ ) and a state of the art triple pass Raman spectrometer with diode array detection. Typical spectra are shown in Fig. 2 (left part).

Because of the low symmetry and the large number of atoms in the unit cell, the spectra show a large number of active phonon modes in all symmetries. What immediately draws attention is the large width of most of the observed phonon modes. Particularly in the  $400\text{--}800\ \text{cm}^{-1}$  region, the line widths are  $10\text{--}50\ \text{cm}^{-1}$ . The active phonons here are expected to be

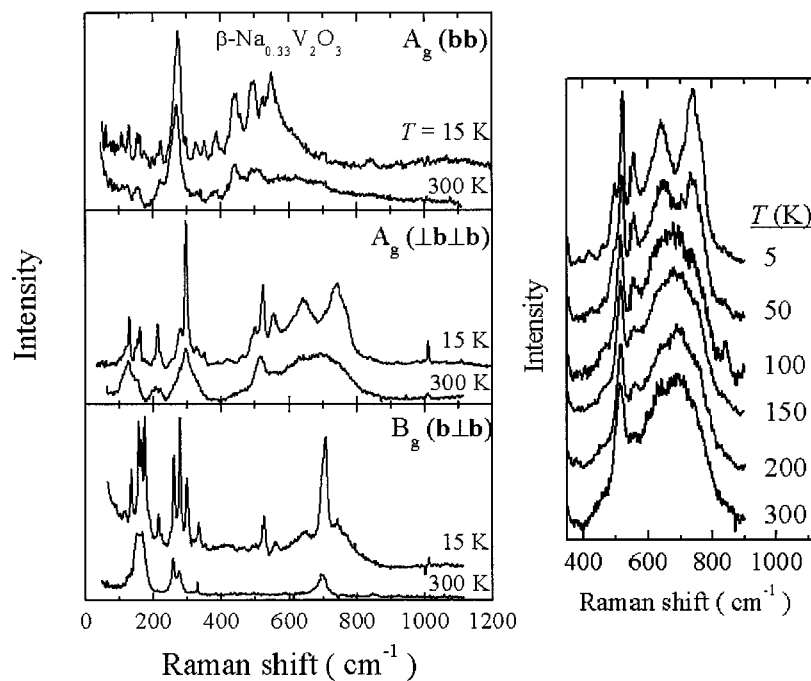


**Fig. 2.** *Left:* Polarized Raman spectra of  $\beta\text{-Na}_{0.33}\text{V}_2\text{O}_3$  for  $T = 15\ \text{K}$  and  $300\ \text{K}$ . Upper panel,  $A_g(\mathbf{bb})$ ; middle panel,  $A_g(\mathbf{lb|lb})$ ; lower panel,  $B_g(\mathbf{b|b})$  symmetry. *Right:* Detailed temperature dependence of the  $400\text{--}800\ \text{cm}^{-1}$  region of the  $A_g(\mathbf{lb|lb})$  Raman spectrum. In all panels the subsequent curves have been given an offset for clarity.

vanadium–oxygen bending modes. This strong broadening is believed to be due to a strong electron–phonon coupling, consistent with a polaronic picture of the electronic properties of this material [8,9]. The coupling is then a result of the modulation of the hopping parameters for O(2p)—V(3d) hopping by the phonons.

A group theoretical analysis shows that the room temperature  $k = 0$  optical phonons can be classified as  $\Gamma = 11A_u + 22B_u + 20A_g + 10B_g$ , in which the *gerade* modes are Roman active ( $A_g$  in  $(aa)$ ,  $(bb)$ ,  $(cc)$ , and  $(ac)$ , and  $B_g$  in  $(ab)$  and  $(bc)$  polarization) and the *ungerade* IR active ( $A_u$  for b polarization,  $B_u$  for a and c polarizations). Consistent with the crystal symmetry 16 modes are observed in  $A_g$  symmetry, and 9 in  $B_g$  symmetry. The missing modes might be too weak to be observed, but might also escape detection because of near degeneracy.

Below the sodium ordering transition the crystal structure adheres to a  $C_{2h}^5$  symmetry [6,10]. The symmetry analysis leads now to a decomposition  $\Gamma = 65A_u + 64B_u + 66A_g + 66B_g$  for the optical modes. Experimentally 55 modes are observed in  $A_g$  symmetry, and 20 in  $B_g$  symmetry. Below the charge ordering transition the unit cell triples, leading to about 190 active phonons for each irreducible representation. Although a few phonons seem to be activated below the metal insulator transition, the spectra do not show this tripling. Again, this might be due to a lack of scattering strength or near degeneracies.

The strongest changes in the spectra are observed below the MIT at  $T = 136$  K. This is exemplified in Fig. 5 (right panel). Apparently, the localization of the electrons leads to a decrease of the coupling of the phonons to electronic excitations.

#### 4. OPTICAL SPECTROSCOPY

Temperature-dependent optical spectra of  $\beta\text{-Na}_{0.33}\text{V}_2\text{O}_3$  in the NIR–UV range ( $6000\text{--}35000\text{ cm}^{-1}$ ) have been measured using ellipsometry on a surface containing the  $b$ -axis. In addition, the reflectivity spectra have been measured as a function of temperature and polarization in the IR–MIR range ( $20\text{--}6000\text{ cm}^{-1}$ ). The optical conductivity of  $\beta\text{-Na}_{0.33}\text{V}_2\text{O}_3$  has been determined by combining the reflectivity data with the ellipsometric data and performing a Kramers–Kronig analysis [9]. The room temperature results are shown in Fig. 3.

The strong absorption band observed above  $10,000\text{ cm}^{-1}$  in both spectra is due to charge transfer excitations from the oxygen 2p to the vanadium 3d

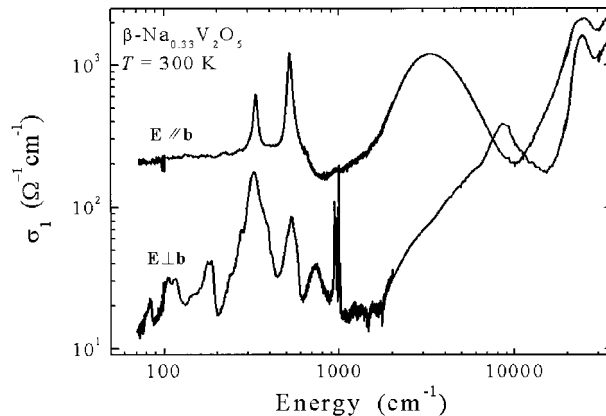


**Fig. 3.** Optical conductivity of  $\beta\text{-Na}_{0.33}\text{V}_2\text{O}_3$  at room temperature calculated from reflectivity spectra (FIR–MIR) and ellipsometric data (MIR–UV) [9].

levels, similar as has been observed in  $\alpha\text{-Na}_{0.33}\text{V}_2\text{O}_3$  [11]. The optical conductivity perpendicular to the  $b$ -axis shows an absorption band around  $8000\text{ cm}^{-1}$ , again similar to what is observed in  $\alpha\text{-NaV}_2\text{O}_3$ . This band is probably due to a bonding–antibonding transition on the  $V_1\text{—O—}V_3$  bonds [9].

At lower energy the 1D metallic nature of  $\beta\text{-Na}_{0.33}\text{V}_2\text{O}_3$  is clearly demonstrated by the finite spectral weight for  $E \rightarrow 0$  for a polarization along the  $b$ -axis, and the tendency to zero weight in the perpendicular polarization. Indeed the data parallel to  $b$  may be fitted by a Drude model, yielding an unscreened plasma frequency of  $\simeq 3200\text{ cm}^{-1}$ , and a scattering time  $\tau \simeq 40$  ps. This low energy response has been attributed to mobile small polarons. From the optical data the estimated DC conductivity is  $200\text{ }\Omega^{-1}\text{ cm}^{-1}$ , which compares well to the published DC conductivity of  $100\text{ }\Omega^{-1}\text{ cm}^{-1}$  [1]. Another manifestation of the polaronic nature of  $\beta\text{-Na}_{0.33}\text{V}_2\text{O}_3$  is found in the characteristic [12] absorption peak around  $3000\text{ cm}^{-1}$ .

At room temperature one expects a total of 32 active phonon modes, 11 in  $A_u$  symmetry (polarization along  $b$ ), and 22 in  $B_u$  symmetry ( $\perp b$ ). Along the insulating direction (Fig. 3, lower curve) we indeed observe 22 active phonon modes. In contrast, the metallic direction (figure 5, upper curve) exhibits only two strong phonon modes, all other modes appear as strongly broadened weak features in the spectrum, indicating again the importance of electron–phonon coupling in this material. Already below the sodium ordering transition one expects many new phonon modes, though only a few are actually observed (for an example see Fig. 4 lower right panel). In contrast, the MIT leads to a spectacular gradual appearance

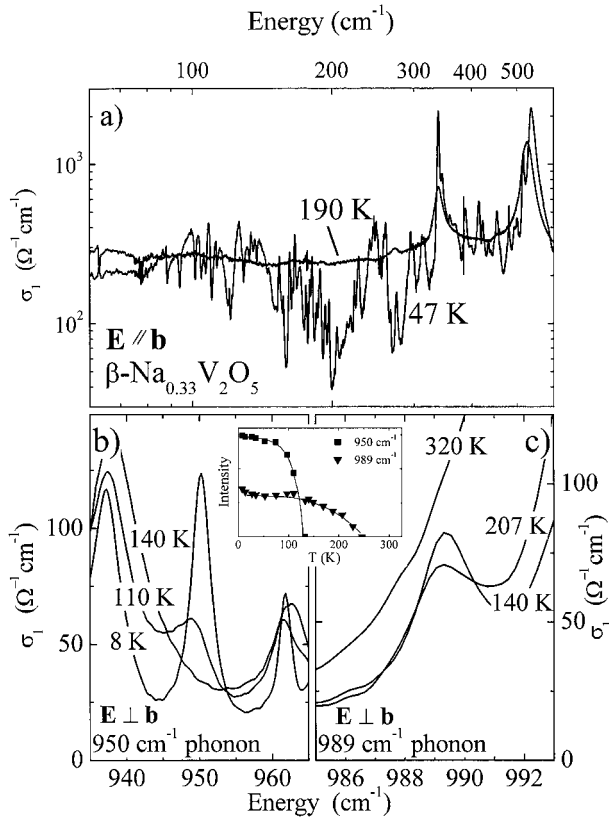


**Fig. 4.** Upper panel: Optical conductivity of  $\beta\text{-Na}_{0.33}\text{V}_2\text{O}_5$  along the metallic direction above and below the charge ordering transition. Lower panels: Phonon modes appearing below the sodium (c) and charge ordering (b) transitions. The inset shows the temperature dependence of the phonons shown in panels (b) and (c).

of a large number of phonon modes (see Fig. 4, upper and lower left panels). The observed behavior is reminiscent of the observation of phase or charged phonons in several charge density wave materials, resulting from electron–phonon interactions [13].

## 5. CONCLUSIONS

The Raman and optical spectra presented in this contribution demonstrate in many ways the importance of electron–phonon coupling in  $\beta\text{-Na}_{0.33}\text{V}_2\text{O}_5$ .

The observed phonon modes and symmetry are found to be in overall agreement with the phase transitions in this material, although the appearance of the many modes in the IR spectra along the metallic direction probably does not result from symmetry breaking, but rather gain strength from electron–phonon coupling in the charge ordered phase. Finally, one interesting undiscussed aspect of the optical data is the appearance of a continuum and Fano distortions of phonon modes (see Fig. 4 upper panel). The origin of this low-energy continuum is presently unknown, but likely to be of electronic nature.

## ACKNOWLEDGMENTS

This work was partially supported by the Dutch Foundation for Fundamental Research on Matter (FOM) and by INTAS (99-155).

## REFERENCES

1. H. Yamada and Y. Ueda, *J. Phys. Soc. Jpn.* **68**, 2735 (1999).
2. T. Yamauchi, Y. Ueda, and N. Mōri, *Phys. Rev. Lett.* **89**, 057002-1 (2002).
3. A. D. Wadsley, *Acta Cryst.* **8**, 695 (1955).
4. H. Kobayashi, *Bull. Chem. Soc. Jpn.* **52**, 1315 (1979).
5. K. Maruyama and H. Nagasawa, *J. Phys. Soc. Jpn.* **48**, 2159 (1980).
6. J.-I. Yamaura, M. Isobe, H. Yamada, T. Yamauchi, and Y. Ueda, *J. Phys. Chem. Solids* **63**, 957 (2002).
7. A. N. Vasil'ev, I. Marchenko, A. I. Smirnov, S. S. Sosin, P. L. Kapitza, H. Yamada, and Y. Ueda, *Phys. Rev. B* **64**, 174403 (2001).
8. N. F. Mott, *Metal–Insulator Transitions* (Taylor and Francis, London, 1974).
9. C. Pressura, M. Popinciuc, P. H. M. van Loosdrecht, D. van der Marel, M. Mostovoy, G. Maris, T. T. M. Palstra, H. Yamada, and Y. Ueda, 2002; unpublished manuscript (2002).
10. G. Maris *et al.*, private communication (2002).
11. C. Pressura, D. van der Marel, M. Dischner, C. Geibel, and R. K. Kremer, *Phys. Rev. B* **62**, 16522 (2000).
12. C. A. Kuntscher, M. Dressel, F. Lichtenberg, J. Mannhart, D. van der Marel, Y. Kanai, S. Kagoshima, and H. Nagasawa (2002); *Preprint cond-mat/0205049*; D. Emin, *Phys. Rev. B* **48**, 13691 (1993); D. Kaplan and A. Zylbersztejn, *J. de Physique* **37**, L-123 (1976).
13. M. J. Rice, *Phys. Rev. Lett.* **37**, 36 (1976); L. Degiorgi, P. Wachter, and C. Schlenker, *Physica B* **164**, 305 (1990), and references therein.